

Received February 15, 2019, accepted February 26, 2019, date of publication March 11, 2019, date of current version April 2, 2019.

Digital Object Identifier 10.1109/ACCESS.2019.2904145

A Hybrid Feature Extraction Method With Regularized Extreme Learning Machine for Brain Tumor Classification

ABDU GUMAEI^{ID1}, MOHAMMAD MEHEDI HASSAN^{ID2}, (Senior Member, IEEE),

MD RAFIUL HASSAN³, ABDULHAMEED ALELAIWI⁴, (Member, IEEE),

AND GIANCARLO FORTINO^{ID5}, (Senior Member, IEEE)

¹Computer Science Department, College of Computer and Information Sciences, King Saud University, Riyadh 11543, Saudi Arabia

²Information Systems Department, College of Computer and Information Sciences, King Saud University, Riyadh 11543, Saudi Arabia

³Information and Computer Science Department, King Fahd University of Petroleum and Minerals, Dhahran 31261, Saudi Arabia

⁴Software Engineering Department, College of Computer and Information Sciences, King Saud University, Riyadh 11543, Saudi Arabia

⁵Department of Informatics, Modeling, Electronics and Systems, University of Calabria, 87036 Rende, Italy

Corresponding author: Mohammad Mehedi Hassan (mmhassan@ksu.edu.sa)

This work is supported by the Deanship of Scientific Research at King Saud University through Research Group Project RGP-318.

ABSTRACT Brain cancer classification is an important step that depends on the physician's knowledge and experience. An automated tumor classification system is very essential to support radiologists and physicians to identify brain tumors. However, the accuracy of current systems needs to be improved for suitable treatments. In this paper, we propose a hybrid feature extraction method with a regularized extreme learning machine (RELM) for developing an accurate brain tumor classification approach. The approach starts by preprocessing the brain images by using a min–max normalization rule to enhance the contrast of brain edges and regions. Then, the brain tumor features are extracted based on a hybrid method of feature extraction. Finally, a RELM is used for classifying the type of brain tumor. To evaluate and compare the proposed approach, a set of experiments is conducted on a new public dataset of brain images. The experimental results proved that the approach is more effective compared with the existing state-of-the-art approaches, and the performance in terms of classification accuracy improved from 91.51% to 94.233% for the experiment of the random holdout technique.

INDEX TERMS Brain tumor classification, hybrid feature extraction, NGIST features, PCA, regularized extreme learning machine.

I. INTRODUCTION

Brain is the management center in the human body. It is responsible to execute all activities throughout a large number of connections and a huge number of neurons. Brain tumor is one of the most serious diseases, occurred due to an abnormal growth of cells in the brain, affecting the functions of the nervous system. There are different types of brain tumors, which can be either malignant or benign. The early stage of tumor detection depends on the physician's knowledge and experience, making the patients have a chance to recover his life and survival [1]. An automated classification system of brain tumors is an effective tool for supporting the physicians to follow a successful treatment option. Such system

The associate editor coordinating the review of this manuscript and approving it for publication was Victor Hugo Albuquerque.

uses the images captured by magnetic resonance (MR) imaging devices, which are widely used by the radiologists of brain diagnosis [2]. In recent years, several studies have been proposed and different automated systems have been developed for detecting and classifying brain tumors using MR images. For instance, Sompong and Wongthanavasu [3] proposed a method for brain tumor segmentation based on a hybrid of fuzzy c-means algorithm and cellular automata. In this method, the seed-growing problem of segmentation methods is solved by using a new similarity function with a gray level co-occurrence matrix (GLCM) and evaluated on BraTS2013 dataset. Sehgal *et al.* [4] proposed an automated method for detecting brain tumor based on image segmentation and tumor extraction. The authors utilized the circularity feature and the area to extract the tumor from segmented brain images. The authors validated their methods by comparing

their segmented images with the ground truth images and achieved an average of 0.729 (i.e., 72.9%) similarity. In [5], the authors developed a semi-automatic technique for MR brain image segmentation based on human interaction to generate a feature map from MR images and used it to initialize the active contour model for segmenting the region of interest (ROI) area. Overlap index parameter and Jaccard coefficient are used to compare the results with ground truth ROI images, which are manually segmented from the original images. Praveen and Agrawal [6] proposed a multi-stage approach which detects brain tumor from MR images using a set of steps, including image preprocessing through cropping, noise reduction, scaling, and histogram equalization; feature extraction using histogram and GLCM techniques; and classification using random forest (RF) classifier. A dataset of 120 patients are utilized to test this approach and they achieved 87.62% of classification accuracy. In another work [7], the authors proposed a wavelet-based method to extract features from MR images. In this method, segmentation of brain MR images was performed using a Markov random field (MRF) model. Abbasi and Tajeripour [8] presented an automatic detection method to detect brain tumor from 3D images. The ROI was segmented from the image's background using bias field correction and histogram matching. After that, the RF method was used for brain tumor detection. This method was evaluated using the BRATS 2013 dataset. Classification of brain tumors from computed tomography (CT) images using deep learning methods such as multiple convolutional neural networks (CNNs) with discrimination method [9], [10] and single CNN method [11] have also been proposed. In [12]–[14], the authors introduce a CNN architecture to classify brain tumors. In this architecture, CNN extracts the features from the pixels of input brain image through two main operations: convolution and pooling. Recently, Ari and Hanbay [15] proposed a deep learning method to classify brain tumor either to malignant or benign using extreme learning machine local receptive fields (ELM-LRF). This method was evaluated on a dataset that consists of images collected from sixteen patients. Among them images of nine patients were used for training and seven patients were used for testing. Even though deep learning methods improve the classification of brain tumors, they need a large amount of training samples and a high cost of computation, and they take a long time for training [16].

Regularized Extreme learning machine (RELM) is a classification and regression method, used in many applications due to its ability to overcome some disadvantages related to the backpropagation method [17]. The speed of training and low complexity makes the RELM advantageous over the other classifiers.

The main contributions of this work are outlined in the following lines:

- We propose an automatic approach for brain tumor classification in order to aid the radiologists and physicians in order to identify the type of brain tumors.

- We propose a novel and effective hybrid feature method referred to as PCA-NGIST that uses Normalized GIST descriptor with PCA to extract the significant features from brain images without using any kind of image segmentation. It should be noted that, image segmentation methods are affected by changes in illumination and shadowing leading to inaccurate results in brain tumor classification.
- We use a RELM classifier due to its regularization property to reduce the overfitting problem and its speed for training.
- We optimize the parameters of the proposed approach using a grid search algorithm.
- We evaluate the proposed approach using a new public dataset of brain images and compare with the state-of-the-art approaches on the same dataset.

The rest of the paper is organized as follows: proposed approach is given in Section II, experiments and discussions are reported in Section III, and finally a conclusion is summarized in Section IV.

II. PROPOSED APPROACH

In this section, we describe the proposed approach. Our approach consists of three steps: (A) Brain image preprocessing, (B) Brain feature extraction, and (C) Brain tumor classification. The input of the approach is the brain images and the output is the respective type of the brain tumor. Figure 1 shows the flowchart of the proposed approach. The details of the steps of our proposed approach are described in the subsections below.

A. BRAIN IMAGE PREPROCESSING

Brain image preprocessing is an important step, which has a positive effect on the result of brain image analysis and the quality of brain feature extraction. After reading the input brain images, these images have large values which are outside of the range [0, 255], including negative values. Therefore, this step in our approach transforms the brain images into intensity brain images in the range [0, 1] by using a min-max normalization rule as given in the equation below:

$$f(x, y) = \frac{f(x, y) - V_{min}}{V_{max} - V_{min}} \quad (1)$$

where $f(x, y)$ represents each pixel in the brain image, V_{min} and V_{max} are the minimum value and maximum value in the image (f).

As a result, the contrast of brain edges and regions will be enhanced and improved. Figure 2 shows an example of the input and output of this step.

B. BRAIN FEATURE EXTRACTION

1) GIST DESCRIPTOR

GIST is a feature descriptor, first proposed by Olive and Torralba [18] for scene classification. It defines the scene features based on the spatial envelope (low dimensional representation) of the image [18]. These features represent the

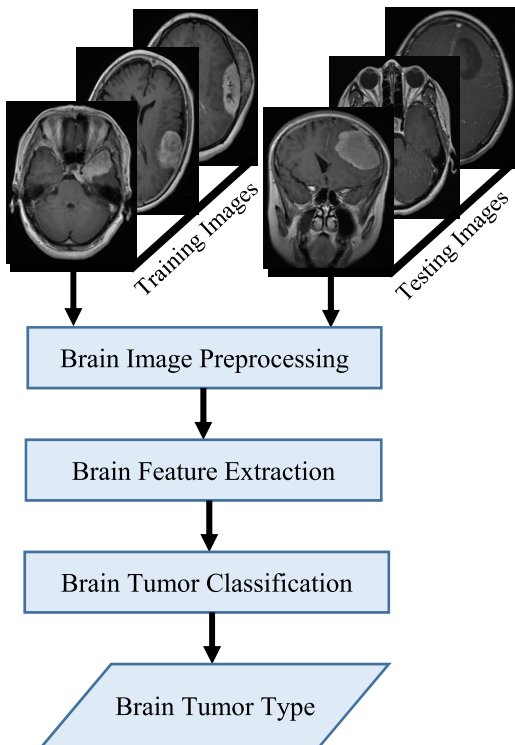


FIGURE 1. Proposed approach flowchart.

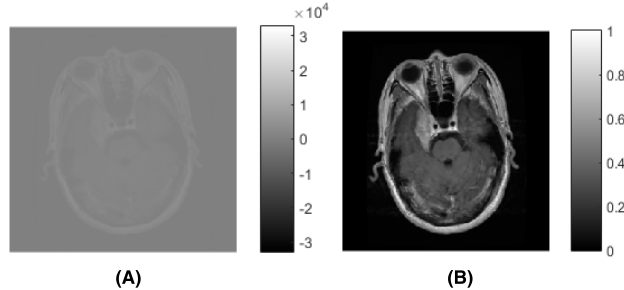


FIGURE 2. The input and output of image preprocessing step; (A) An input image of brain raw data values and (B) An output image of brain data intensity values.

dominant spatial structure of the image which are computed by convolving the input image with Gabor filter at m scales and n orientations, generating $m \times n$ filtered images of the same input image size; then, dividing each filtered image into 4×4 grid; after that, computing the average value within each grid; and finally, concatenating the 4×4 grid averaged values of all $m \times n$ filtered images, producing in a total of $m \times n \times 4 \times 4$ GIST feature vectors.

2) HYBRID PCA-NGIST METHOD

The hybrid PCA-NGIST is a PCA-based normalized GIST feature extraction method which combines the PCA method with GIST descriptor after normalizing it using L_2 norm. Normalized GIST (NGIST) descriptor is an improved version of traditional GIST descriptor, proposed by Gumaei *et al.* [19], [20]. The NGIST can solve the problem of changes in images' illumination and shadowing by

normalizing them using L_2 norm. It can be defined as a low dimensional representation, used to summarize the orientations and scales of images, providing a rough description of normalized features without using any form of segmentation [18]. While the PCA is a common feature extraction and reduction method, exploited to generate a new compact set of significant features from the original GIST features, preserving the classification step from overfitting problem. The PCA-NGIST method computes the GIST features from the brain images and finds the eigenvectors of these features that have the highest eigenvalues, then projects them into a new feature subspace equal or less dimensions.

Suppose that $f(x, y)$ is a 2D Gabor filter of the brain image at m scales and n orientations, computed as:

$$f(x, y) = \left(\frac{1}{2\pi\sigma_x\sigma_y} \right) \exp \left[-\frac{1}{2} \left(\frac{x^2}{\sigma_x^2} + \frac{y^2}{\sigma_y^2} \right) + 2\pi j\omega x \right] \quad (2)$$

where ω is a radial frequency of Gabor filter, j is a complex number equals $\sqrt{-1}$, and σ_x and σ_y are the complete and non-orthogonal basis of Gabor filter [21].

By using the 2D Gabor filter function $f(x, y)$, the Fourier function transform $F(u, v)$ can be written as follows:

$$F(u, v) = \exp \left\{ -\frac{1}{2} \left[\frac{(u - \omega)^2}{\sigma_u^2} + \frac{v^2}{\sigma_v^2} \right] \right\} \quad (3)$$

where the σ_u and σ_v can be calculated as:

$$\sigma_u = \frac{1}{2}\pi\sigma_x \text{ and } \sigma_v = \frac{1}{2}\pi\sigma_y \quad (4)$$

Considering $f(x, y)$ is a mother function of Gabor wavelet transform, the dictionary of Gabor filter is derived by setting up the orientation (θ) and scaling factor (δ) parameters as:

$$f_{mn}(x, y) = \delta^{-m} f(x', y'), \quad (5)$$

where $\delta > 1$, m and n are integer numbers that represents the scale number and orientation number, $\theta = n\pi/N$ and x', y' are computed as:

$$x' = \delta^{-m} (x \cos \theta + y \sin \theta) \quad (6)$$

$$y' = \delta^{-m} (-x \sin \theta + y \cos \theta) \quad (7)$$

where we consider O is the number of orientations and compute the value of θ as $\theta = n\pi/O$. The scale δ^{-m} in Eq. (4), (5), and (6) is designed to make the energy more independent [21].

To extract brain features, four scales and eight orientations of Gabor filter are applied on brain images. Consequently, we get a 32 of brain images which will be divided into a 4×4 blocks. Then, the average intensity value of each block is computed to get a GIST feature vector (G) that contains a total of $8 \times 4 \times 4 \times 4 = 512$ features [18]–[20]. For obtaining the normalized GIST (NGIST), the feature vectors (G_i) will be normalized based on L_2 norm to mitigate the changes in shadowing and illumination as follows:

$$G_i = \frac{G_i}{\sqrt{\sum_{j=1}^{512} |G_j|^2}} \quad (8)$$

Supposing that T is a matrix of $\mathcal{N} \times 512$ contains a set of NGIST brain feature vectors (G_i). For reducing the redundancy among these feature vectors, a PCA is adopted as unsupervised learning algorithm to compute the matrix of selected eigenvectors ($EV_{512 \times K}$). These eigenvectors will be used later to project $T_{N \times 512}$ into a new compact feature matrix, $Y_{N \times K}$ by the following equation [22]:

$$Y_{N \times K} = T_{N \times 512} \cdot EV_{512 \times K} \quad (9)$$

The steps of PCA algorithm to calculate the $EV_{512 \times K}$ are given in the following: Suppose that L is number of brain tumor classes in training dataset (T) of N NGIST vectors $\{G_1, G_2, \dots, G_N\}$, where $G_i \in \text{RealNumber}$; each training vector belongs to a class $j \in \{1, 2, \dots, L\}$. The covariance matrix is defined as:

$$S = \frac{1}{N-1} \sum_{i=1}^N (G_i - \bar{G}) \cdot (G_i - \bar{G})^T \quad (10)$$

where \bar{G} is the average of all training data vectors and calculated as:

$$\bar{G} = \frac{1}{N} \sum_{i=1}^N G_i \quad (11)$$

The K eigenvectors ($EV_{512 \times K}$) can be selected from the original eigenvectors matrix ($EV_{512 \times 512}$) corresponding to the top K eigenvalues resulted from the decomposition of covariance matrix (S), which represented as follows:

$$EV_{512 \times K} = EV(i, j), \quad (12)$$

where $i = 1, \dots, 512$ and $j = 1, \dots, K$.

C. BRAIN TUMOR CLASSIFICATION

Brain tumor classification is the final step of the proposed approach, that is used to identify the type of brain tumor based on the RELM classifier. RELM is a feedforward neural networks (FNNs), composed of input and output layers, as well as a single hidden layer. Initializing the weights and biases of the input layer is randomly selected before going to compute the weights of the output layer [23], [24]. The concept of ELM to classify multiclass problem is introduced by Huang et al. [25] in more detail. In this step and during the training phase, the RELM classifier model is trained on the brain features obtained from the previous step. Subsequently, the trained RELM model is utilized to classify the type of brain tumor in an effective manner. Algorithm 1 illustrates the input and output of this step.

III. EXPERIMENTS AND DISCUSSIONS

A. DATASET

The dataset used in this study provided by Cheng [26], [27]. It contains 3064 brain tumor MRI images. The images were taken from 233 patients at different planes: transverse plane, lateral plane, and frontal plane. These images were grouped into three sets: 994 axial images, 1025 sagittal images, and 1045 coronal images. There are three types of brain tumors in the dataset: meningioma (1426 images),

Algorithm 1 Brain Tumor Classification

Input: Parameters,

Training dataset and testing dataset of extracted brain features,
Training labels.

Output: Testing labels (l_j)

Begin

1. Training-phase:

1.1. Weights and biases initialization

1.1.1. Selecting randomly the weights (w_i) and biases (b_i) of the inputs (x_i) for the RELM's input layer

1.2. Matrix computation

1.2.1. Calculating the hidden layer matrix (H) using Eq. (13) as bellow:

$$H = \begin{bmatrix} g(w_1 \cdot x_1 + b_1) & \cdots & g(w_M \cdot x_1 + b_M) \\ \vdots & \cdots & \vdots \\ g(w_1 \cdot x_N + b_1) & \cdots & g(w_M \cdot x_N + b_M) \end{bmatrix}_{N \times M} \quad (13)$$

1.2.2. Calculating the weight and target matrices (β and T) using Eq. (14).

$$\beta = \begin{bmatrix} \beta_1^T \\ \vdots \\ \beta_M^T \end{bmatrix} \quad \text{and} \quad T = \begin{bmatrix} t_1^T \\ \vdots \\ t_N^T \end{bmatrix} \quad (14)$$

2. Testing-phase:

2.1. Matrix computation

2.1.1. Calculating the hidden layer matrix (\hat{H}) using Eq. (13).

2.1.2. Computing the output weights using Eq. (15).

$$\hat{\beta} = (H^T H + \lambda I)^{-1} H^T T \quad (15)$$

2.1.3. Computing the output matrix (O_j) using Eq. (16).

$$O_j = \hat{H} \hat{\beta} \quad (16)$$

2.1.4. Finding the testing class label (l_j), where $j \in L$ and L is the number of classes by using Eq. (17).

$$l_j = \arg \max_{j \in L} (O_j) \quad (17)$$

Return Testing labels (l_j)

End

glioma (708 images), and pituitary (930 images). Each image contained an original size of 512 x 512 in pixels. The owner of this dataset organized the brain images, labels, patient ID, tumor mask images, and tumor border coordinates in MATLAB data format. Examples of the dataset images are shown in Figure 3.

B. PARAMETER SETTINGS

There are some parameters of the proposed approach that need to be initialized. During the experiments, the values of

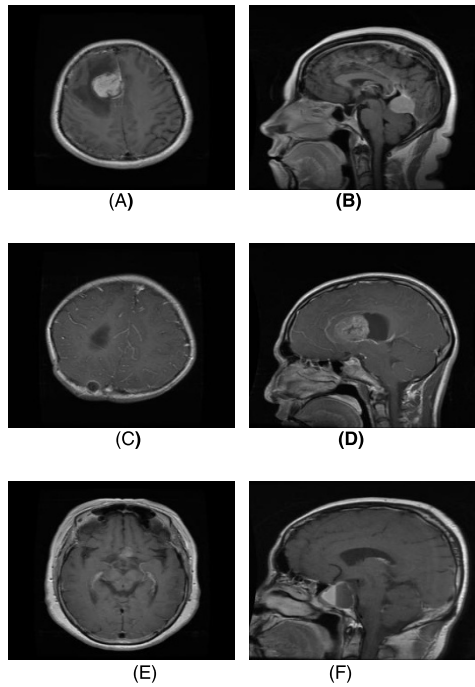


FIGURE 3. Example of brain T1 images taken from the dataset; (A) - (B) Meningioma brain tumor; (C) - (D) Glioma brain tumor; and (E) - (F) Pituitary brain tumor.

TABLE 1. Parameter settings.

Method	Parameters
PCA-NGIST	Image Size = $256 \times 256 = 65,536$ pixels. Number of Orientations = 8 Number of Scales = 4 Block Size = $4 \times 4 = 16$ pixels. The number of Eigenvectors is: $EV \in \{50, 150, 250, 350\}$.
RELM	The number of Hidden Nodes is: $M_{RELM} \in \{1500, 1005, 1010, \dots, 2000\}$. Size of RELM grid search=21 The regularization parameter is: $(\lambda) = \exp(val)$, where $val \in \{-10, -9.8, -9.6, \dots, 9.8, 10\}$ The activation function is a TANH function, $\tanh(x) = \left(\frac{e^x - e^{-x}}{e^x + e^{-x}} - 1 \right)$.

these parameters are selected using the grid search algorithm and our knowledge in image processing and machine learning fields. Table 1 states the parameter values that were used in our experiments. As mentioned above, some parameters of the approach were chosen empirically. For example, we ran the experiments using different number of eigenvectors and RELM's hidden nodes and then selected the number of eigenvectors which produces an optimal representative features and the number of RELM's hidden nodes that achieves a high accuracy.

C. EXPERIMENTAL RESULTS

A number of experiments are conducted based on holdout and 5-folds cross validation techniques. In the holdout technique, we divided the dataset into two sets: a training set which

contains 70% of the dataset, and a testing set that contains 30% of the dataset. On the other hand, in the 5-folds cross validation, the dataset is divided into five sets; one of them is selected for testing and the remaining four sets are used for training, and this is done for five times. For evaluation, the confusion matrices of the actual and classified brain tumor classes are computed among the testing phase.

	Meningioma	Glioma	Pituitary
Meningioma	167	20	13
Glioma	28	403	2
Pituitary	5	4	277
Accuracy	92.165%		

(A)

	Meningioma	Glioma	Pituitary
Meningioma	176	17	7
Glioma	26	406	1
Pituitary	3	5	278
Accuracy	93.58%		

(B)

	Meningioma	Glioma	Pituitary
Meningioma	178	16	6
Glioma	26	407	0
Pituitary	4	6	276
Accuracy	93.689%		

(C)

	Meningioma	Glioma	Pituitary
Meningioma	177	16	7
Glioma	20	413	0
Pituitary	6	4	276
Accuracy	94.233%		

(D)

FIGURE 4. results of confusion matrices; (A) A confusion matrix of PCA-NGIST with RELM (EVS = 50) - (B) a confusion matrix of PCA-NGIST with RELM (EVS = 150); (C) a confusion matrix of PCA-NGIST with RELM (EVS = 250); AND (D) A confusion matrix of PCA-NGIST with RELM (EVS = 350).

Figure 4 shows the confusion matrices of brain tumors classification obtained using different Eigenvectors (EVs) of PCA for the holdout technique.

From these matrices, the accuracy results are calculated as:

$$\text{Accuracy} = \frac{(TP + TN)}{(TP + FP + TN + FN)} \quad (18)$$

where FP and TP represent false and true positive rates; FN and TN denote false and true negative rates.

Figure 5 demonstrates the accuracy results of brain tumors classification at different numbers of EVs and RELM's hidden nodes.

From the Figure 5, we notice that the best EVs value is equal to 350. Therefore, this value will be fixed and selected to represent the significant extracted features from brain images.

In the Figure 6, we see the performance of PCA-NGIST with RELM classifier compared to the other related approaches. We also noticed that the classification performance in terms of accuracy using NGIST descriptor is better than the classification accuracy of using GIST.

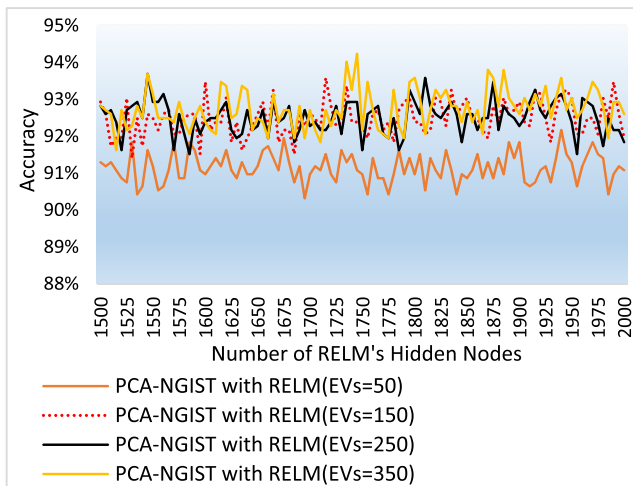


FIGURE 5. Example of brain T images taken from the dataset; (A) - (B) Meningioma brain tumor; (C) - (D) Glioma brain tumor; and (E) - (F) Pituitary brain tumor.

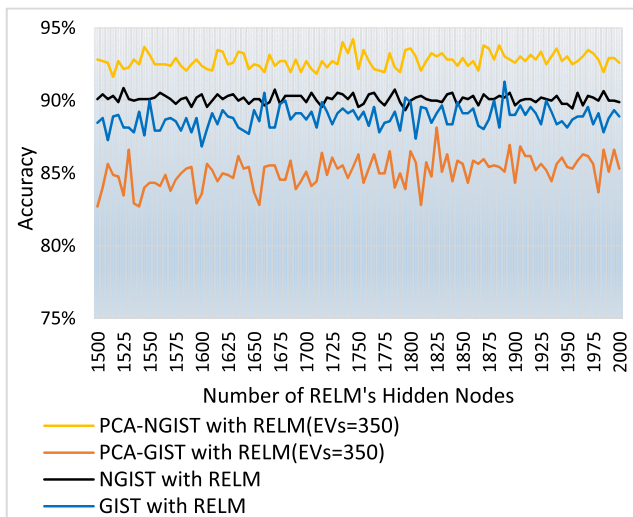


FIGURE 6. Example of brain T Images taken from the dataset; (A) - (B) Meningioma brain tumor; (C) - (D) Glioma brain tumor; and (E) - (F) Pituitary brain tumor.

	Meningioma	Glioma	Pituitary
Meningioma	113	15	4
Glioma	5	283	0
Pituitary	3	4	185
Accuracy	94.935%		

FIGURE 7. Example of brain T images taken from the dataset; (A) - (B) Meningioma brain tumor; (C) - (D) Glioma brain tumor; and (E) - (F) Pituitary brain tumor.

Another experiment is also done using the 5-folds cross validation method. The classification accuracies for the five different testing sets are in the range between 91.667% and 94.935% and with average accuracy is 92.6144%. The confusion matrix which has maximum classification accuracy is shown in Figure 7.

TABLE 2. Comparison of brain tumor classification accuracy using the proposed approach against using the state-of-the-arts.

Reference	Approach	Image Size	Accuracy (%)
[13]	CNN	256 x 256	91.43
[13]	RF	256 x 256	90
[14]	CNN	64 x 64	84.19
This Study	SVM-RBF	256 x 256	91.51
	DT	256 x 256	84.33
	NB Naïve	256 x 256	66.92
	Proposed PCA-NGIST with RELM	256 x 256	94.233

To evaluate the proposed approach, Table 2 lists the classification accuracy of our proposed approach against that of using the state-of-the-art approaches.

We can see that the classification accuracy achieved using our proposed approach is better than the accuracy of using the state-of-the-arts techniques (e.g., CNN, SVM-RBF, and NB). The reason for this improvement in classification accuracy is due to the ability of extracting the influential features in decrementing the type of brain tumors using the novel hybrid feature extraction method.

IV. CONCLUSIONS AND FUTURE WORK

This paper introduced an effective brain tumor classification approach which has three main steps. At first, brain images are transformed into intensity values using a preprocessing step. Then, the most important features are extracted using a novel and efficient hybrid method, referred to as PCA-NGIST. Finally, brain tumors are classified using RELM classifier.

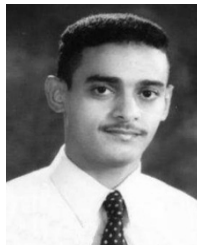
Classification accuracy of the proposed approach is evaluated and compared using a new public dataset of brain tumor images. This dataset contains 3064 brain images with three types of brain tumors, taken from 233 patients. The experiments are performed using holdout (70% training and 30% testing) and 5-folds cross validation techniques.

The experimental results demonstrated that the accuracy of the proposed PCA-NGIST feature extraction method is better than using PCA-GIST, GIST, NGIST methods. Additionally, the results showed that the proposed approach attained high classification rates compared with the state-of-the-arts. We plan to apply the proposed approach in order to solve another biomedical classification problem and perform a comparative study on other machine learning classifiers.

REFERENCES

- E. Dandil, M. Çakiroğlu, and Z. Ekşi, “Computer-aided diagnosis of malign and benign brain tumors on MR images,” in *ICT Innovations: Advances in Intelligent Systems and Computing*, vol. 311. Cham, Switzerland: Springer, 2015, pp. 157–166.
- S. Pereira, A. Pinto, V. Alves, and C. A. Silva, “Brain tumor segmentation using convolutional neural networks in MRI images,” *IEEE Trans. Med. Imag.*, vol. 35, no. 5, pp. 1240–1251, May 2016.

- [3] C. Sompong and S. Wongthanavasu, "Brain tumor segmentation using cellular automata-based fuzzy c-means," in *Proc. 13th Int. Joint Conf. Comput. Sci. Softw. Eng. (JCSSE)*, Khon Kaen, Thailand, Jul. 2016, pp. 1–6.
- [4] A. Sehgal, S. Goel, P. Mangipudi, A. Mehra, and D. Tyagi, "Automatic brain tumor segmentation and extraction in MR images," in *Proc. Conf. Adv. Signal Process. (CASP)*, Pune, India, Jun. 2016, pp. 104–107.
- [5] S. A. Banday and A. H. Mir, "Statistical textural feature and deformable model based MR brain tumor segmentation," in *Proc. 6th Int. Conf. Adv. Comput., Commun. Inform. (ICACCI)*, Jaipur, India, Sep. 2016, pp. 657–663.
- [6] G. B. Praveen and A. Agrawal, "Multi stage classification and segmentation of brain tumor," in *Proc. 3rd Int. Conf. Comput. Sustain. Global Develop. (INDIACom)*, New Delhi, India, Mar. 2016, pp. 1628–1632.
- [7] A. Ahmadvand and P. Kabiri, "Multispectral MRI image segmentation using Markov random field model," *Signal, Image Video Process.*, vol. 10, pp. 251–258, Feb. 2016.
- [8] S. Abbasi and F. Tajeripour, "Detection of brain tumor in 3D MRI images using local binary patterns and histogram orientation gradient," *Neurocomputing*, vol. 219, pp. 526–535, Jan. 2017.
- [9] X. W. Gao, R. Hui, and Z. Tian, "Classification of CT brain images based on deep learning networks," *Comput. Methods Programs Biomed.*, vol. 138, pp. 49–56, Jan. 2017.
- [10] L. Zhao and K. Jia, "Deep feature learning with discrimination mechanism for brain tumor segmentation and diagnosis," in *Proc. Int. Conf. Intell. Inf. Hiding Multimedia Signal Process. (IHM-MSP)*, Adelaide, SA, Australia, Sep. 2015, pp. 306–309.
- [11] X. W. Gao and R. Hui, "A deep learning based approach to classification of CT brain images," in *Proc. SAI Comput. Conf. (SAI)*, London, U.K., Jul. 2016, pp. 28–31.
- [12] A. İşin, C. Direkoglu, and M. Şah, "Review of MRI-based brain tumor image segmentation using deep learning methods," *Procedia Comput. Sci.*, vol. 102, pp. 317–324, 2016.
- [13] J. Paul, "Deep learning for brain tumor classification," M.S. thesis, Dept. Comput. Sci., Vanderbilt Univ., Nashville, TN, USA, May 2016.
- [14] N. Abiwinanda, M. Hanif, S. T. Hesaputra, A. Handayani, and T. R. Mengko, "Brain tumor classification using convolutional neural network," in *World Congress on Medical Physics and Biomedical Engineering*. Singapore: Springer, 2018, pp. 183–189.
- [15] A. Ari and D. Hanbay, "Deep learning based brain tumor classification and detection system," *Turkish J. Elect. Eng. Comput. Sci.*, vol. 26, no. 5, pp. 2275–2286, 2018.
- [16] G.-B. Huang, Z. Bai, L. L. C. Kasun, and C. M. Vong, "Local receptive fields based extreme learning machine," *IEEE Comput. Intell. Mag.*, vol. 10, no. 2, pp. 18–29, May 2015.
- [17] G.-B. Huang, Q.-Y. Zhu, and C.-K. Siew, "Extreme learning machine: Theory and applications," *Neurocomputing*, vol. 70, pp. 489–501, Dec. 2006.
- [18] A. Oliva and A. Torralba, "Modeling the shape of the scene: A holistic representation of the spatial envelope," *Int. J. Comput. Vis.*, vol. 42, no. 3, pp. 145–175, 2001.
- [19] A. Gumaei, R. Sammouda, A. Malik S. Al-Salman, and A. Alsanad, "An improved multispectral palmprint recognition system using autoencoder with regularized extreme learning machine," *Comput. Intell. Neurosci.*, vol. 2018, May 2018, Art. no. 8041609.
- [20] A. Gumaei, R. Sammouda, A. Malik S. Al-Salman, and A. Alsanad, "Anti-spoofing cloud-based multi-spectral biometric identification system for enterprise security and privacy-preservation," *J. Parallel Distrib. Comput.*, vol. 124, pp. 27–40, Feb. 2019.
- [21] T. S. Lee, "Image representation using 2D Gabor wavelets," *IEEE Trans. Pattern Anal. Mach. Intell.*, vol. 18, no. 10, pp. 959–971, Oct. 1996.
- [22] J. Yang, D. Zhang, A. F. Frangi, and L.-Y. Yang, "Two-dimensional PCA: A new approach to appearance-based face representation and recognition," *IEEE Trans. Pattern Anal. Mach. Intell.*, vol. 26, no. 1, pp. 131–137, Jan. 2004.
- [23] A. Gumaei, R. Sammouda, A. M. Al-Salman, and A. Alsanad, "An effective palmprint recognition approach for visible and multispectral sensor images," *Sensors*, vol. 18, no. 5, p. 1575, 2018.
- [24] G.-B. Huang, X. Ding, and H. Zhou, "Optimization method based extreme learning machine for classification," *Neurocomputing*, vol. 74, nos. 1–3, pp. 155–163, 2010.
- [25] G.-B. Huang, H. Zhou, X. Ding, and R. Zhang, "Extreme learning machine for regression and multiclass classification," *IEEE Trans. Syst., Man, Cybern. B. Cybern.*, vol. 42, no. 2, pp. 513–529, Apr. 2012.
- [26] J. Cheng, "Brain tumor dataset (version 5)," 2017. doi: [10.6084/m9.figshare.1512427.v5](https://doi.org/10.6084/m9.figshare.1512427.v5).
- [27] J. Cheng et al., "Enhanced performance of brain tumor classification via tumor region augmentation and partition," *PLoS One*, vol. 10, no. 12, 2015, Art. no. e0144479.



ABDU GUMAEI received the B.S. degree in computer science from the Computer Science Department, AL-Mustansirya University, Baghdad, Iraq, and the master's degree in computer science from the Computer Science Department, King Saud University, Riyadh, Saudi Arabia, where he is currently pursuing the Ph.D. degree in computer science. He was a Lecturer and taught many courses, such as programming languages, at the Computer Science Department, Taiz University. He has involved in several researches in the field of image processing. He has received a patent from the United States Patent and Trademark Office (USPTO), in 2013. His main areas of interest are software engineering, image processing, computer vision, and machine learning.



MOHAMMAD MEHEDI HASSAN (M'12–SM'18) received the Ph.D. degree in computer engineering from Kyung Hee University, South Korea, in 2011. He is currently an Associate Professor with the Information Systems Department, College of Computer and Information Sciences (CCIS), King Saud University (KSU), Riyadh, Saudi Arabia. He has published over 130 research papers in the journals and conferences of international repute. His research areas of interest are cloud computing, the Internet of Things, cognitive computing, sensor networks, big data, mobile cloud, and publish/subscribe systems. He received the Best Journal Paper Award from the IEEE SYSTEMS JOURNAL, in 2018. He received the Best Paper Award from the CloudComp Conference held at China, in 2014. He also received the Excellence in Research Award from CCIS, KSU, in 2015 and 2016. He has also played the role of the Guest Editor for several international ISI-indexed journals.



MD RAFIUL HASSAN received the Ph.D. degree from the University of Melbourne, in 2007. He was a Research Fellow with the University of Melbourne, from 2008 to 2010. He has been an Associate Professor with the Department of Information and Computer Science, King Fahd University of Petroleum and Minerals (KFUPM), Saudi Arabia, since 2010. He holds two U.S. patents and has published more than 40 papers in reputed journals and conference proceedings.



ABDULHAMEED ALELAIWI (M) received the Ph.D. degree in software engineering from the College of Engineering, Florida Institute of Technology, Melbourne, FL, USA, in 2002. He is currently an Associate Professor with the Software Engineering Department, College of Computer and Information Sciences (CCIS), King Saud University (KSU), Riyadh, Saudi Arabia, where he is also serving as the Vice Dean of the Research Chairs Program. He has authored or co-authored many publications. He has published over 70 research papers in the ISI-indexed journals of international repute. His research interests include software testing analysis and design, cloud computing, multimedia, the Internet of Things, big data, and mobile cloud. He has served as a Technical Program Committee Member in numerous reputed international conferences/workshops.



GIANCARLO FORTINO received the Ph.D. degree in computer engineering from the University of Calabria (Unical), Italy, in 2000, where he is currently a Full Professor of computer engineering with the Department of Informatics, Modeling, Electronics, and Systems. He is a Guest Professor with the Wuhan University of Technology, Wuhan, China, a high-end Expert with HUST, China, and a Senior Research Fellow with the Italian National Research Council ICAR Institute. He is the Director of the SPEME Laboratory, Unical, and the Co-Chair of the Joint Laboratories on IoT established between Unical and WUT and SMU Chinese universities, respectively. He is also the Co-Founder and the CEO of SenSysCal S.r.l., a Unical spinoff focused on innovative IoT systems. He has authored over 400 papers in international journals, conferences, and books. His research interests include agent-based computing, wireless (body) sensor networks, and the Internet of Things. He is currently a member of the IEEE SMCS BoG and the IEEE Press BoG, and the Chair of the IEEE SMCS Italian Chapter. He is a (Founding) Series Editor of the IEEE Press Book Series on Human-Machine Systems, the Editor-in-Chief of the *Springer Internet of Things* series, and an AE of many international journals, such as the IEEE TAC, the IEEE THMS, the IEEE IoTJ, the IEEE SJ, the IEEE SMCM, *Information Fusion*, JNCA, and EAAI.

• • •